



## Biaryl-methoxy isonipecotanilides as potent and selective inhibitors of blood coagulation factor Xa

Gianfranco Lopopolo<sup>a</sup>, Filomena Fiorella<sup>a</sup>, Modesto de Candia<sup>a</sup>, Orazio Nicolotti<sup>a</sup>, Sophie Martel<sup>b</sup>, Pierre-Alain Carrupt<sup>b</sup>, Cosimo Altomare<sup>a,\*</sup>

<sup>a</sup> Dipartimento Farmaco-Chimico, University of Bari, Via E. Orabona 4, I-70125 Bari, Italy

<sup>b</sup> School of Pharmaceutical Sciences, University of Geneva, University of Lausanne, Quai Ernest-Ansermet 30, CH-1211 Geneva 4, Switzerland

### ARTICLE INFO

#### Article history:

Received 14 September 2010

Received in revised form 24 October 2010

Accepted 18 November 2010

Available online 26 November 2010

#### Keywords:

Piperidine-4-carboxamide

Factor Xa inhibitor

Anticoagulant

Thromboembolism

### ABSTRACT

New chloro-substituted biaryl-methoxyphenyl piperidine-4-carboxamides were synthesized and assayed *in vitro* as inhibitors of the blood coagulation enzymes factor Xa (fXa) and thrombin. An investigation of effects of the amidine and isopropyl groups attached at the piperidine nitrogen and 5-(halogenoaryl)isoxazol-3-yl groups as biaryl substituents led us to identify new compounds which proved to be selective fXa inhibitors, with inhibition constants in the low nanomolar range. The most potent compound **21e**, that incorporates 2-Cl-thiophen-5-yl group as the P1 motif and 1-isopropylpiperidine P4 group, inhibited fXa with  $K_i$  value of 0.3 nM and very high selectivity over thrombin and some other tested serine proteases, achieving moderate levels of anticoagulant activity in the low micromolar range, as assessed by the prothrombin time clotting assay ( $PT_2 = 3.30 \mu\text{M}$ ). Based on reliable docking simulations, molecular modeling provided a rationale for interpreting structure–activity relationships. The predicted binding modes highlighted the structural requirements for addressing the subsites S1 and S4 of the fXa enzyme.

© 2010 Elsevier B.V. All rights reserved.

### 1. Introduction

Among the novel antithrombotics in development (Arepally and Ortel, 2006; Krynetskiy and McDonnell, 2007), small-molecule orally available inhibitors of proteases in the blood coagulation cascade, mainly factor Xa (fXa) and thrombin, have shown improved efficacy and lesser side effects, such as bleeding, associated with the currently used therapies (warfarin, heparins) (Mackman, 2008; Weitz and Linkins, 2007), which require continuous monitoring for accurate dosing. Due to its position at the confluence of the intrinsic and extrinsic pathways of the coagulation cascade, fXa has emerged as an attractive target for the development of potent and safer anticoagulant drugs. Together with fVa and calcium ions on a phospholipid surface, fXa forms the prothrombinase complex, which is responsible for the conversion of prothrombin to thrombin, the final effector of coagulation. Despite initial efforts in the discovery of oral anticoagulant drugs focused on the development of small-molecule direct inhibitors of thrombin (i.e., the oral DTIs), recently accumulated evidence has suggested that early inhibition in the coagulation cascade at the level of fXa

may have greater antithrombotic potential (Ansell, 2007). Indeed, fXa inhibitors do not affect the existing levels of thrombin, allowing the small amounts of remaining thrombin after fXa inhibition to activate thrombin receptors and preserve primary haemostatic functions (Leadley, 2001). Preclinical studies suggest that selective inhibitors of fXa may possess a wider therapeutic index than DTIs (Wong et al., 2009). Recent reviews described the various chemotypes that were employed in the evolution of fXa inhibitors (de Candia et al., 2009a; Pinto et al., 2010).

The availability of numerous fXa crystallographic structures, paved the road to the use of structure-based drug design and modeling techniques that have been successfully employed to develop new oral fXa inhibitors (Maignan and Mikol, 2001). These techniques have been critical in achieving both enzyme selectivity and oral bioavailability. FXa contains a serine protease domain in a trypsin-like closed  $\beta$ -barrel fold encompassing the catalytic triad Ser195–His57–Asp102 and two essential subsites, S1 and S4. The most potent inhibitors adopt L-shaped binding conformations, orienting two almost orthogonal P1 and P4 groups to fill the S1 and S4 pockets in the enzyme binding site.

Early fXa inhibitors brought as primary anchoring points benzamide (e.g., otamixaban **1**; Fig. 1), naphtylamidine or other basic groups, which in the protonated form interact with Asp189 at the bottom of the S1 pocket, whereas the P4 aromatic moiety is

\* Corresponding author. Tel.: +39 080 5442781; fax: +39 080 5442230.  
E-mail address: [altomare@farmchim.uniba.it](mailto:altomare@farmchim.uniba.it) (C. Altomare).

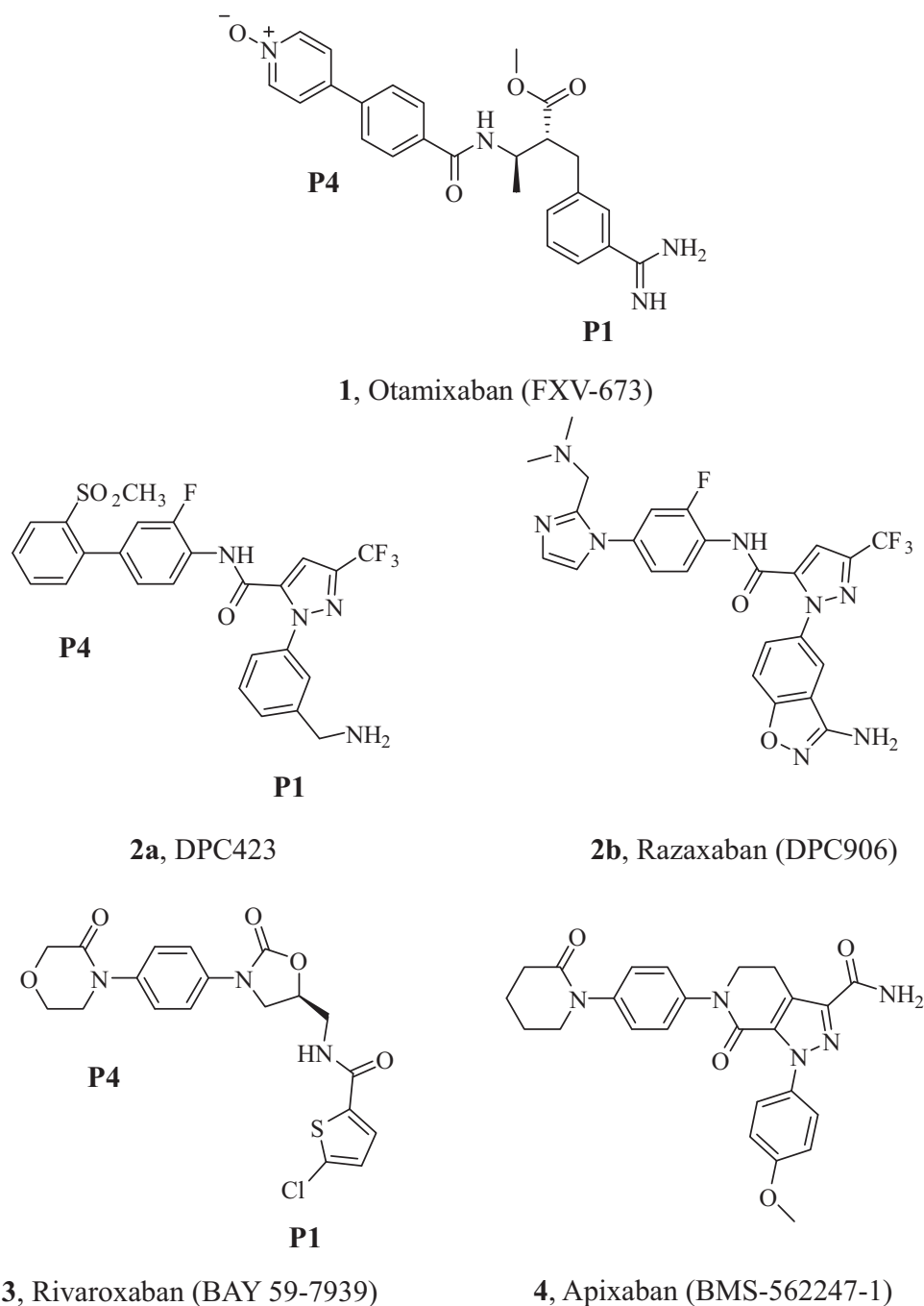


**Fig. 1.** Structures of five representative factor Xa inhibitors – the so-called xabans – bearing as the P1 interacting moiety a basic benzamidine group (otamixaban), less basic amidine isosters (DPC423, razaxaban), and neutral substituted aryl groups (rivaroxaban, apixaban).

embedded into the S4 site, that is an aromatic box lined by the aromatic side chains of Tyr99, Phe174 and Trp215 (Al-Obeidi and Ostrem, 1999). Due to the limited oral bioavailability often associated with the first generation amidine-based fXa inhibitors, efforts were made to replace the amidine group with less basic, such as in DPC423 (**2a**) that was the first oral clinical candidate (Pinto et al., 2001), or nonpolar neutral groups (Lam et al., 2003). These efforts enabled the discovery of second-generation of fXa inhibitors with improved PK properties. They include compounds bearing either less basic amidine isosters, such as razaxaban **2b** (Quan et al., 2005), or neutral P1 substituents, such as rivaroxaban **3** (Roehrig et al., 2005) and apixaban **4** (Pinto et al., 2007) (Fig. 1).

The chlorothiophene moiety in rivaroxaban is buried inside the S1 pocket, with chlorine pointing towards the center of the Tyr228 aromatic ring. The gain in binding energy due to this hydrophobic contact, that is the so-called chloro binding mode, balances the lack of electrostatic/H-bond interactions between amidine and Asp189. Interestingly, it has been shown that even in the presence of a benzamidine plus a chloroaryl or chloroheteroaryl group, fXa-selective inhibitors engage the enzyme binding site by orienting the neutral group into the S1 pocket (Lumma et al., 1998). A similar binding pose has been reported for apixaban **4**, with the 4-methoxyphenyl substituent occupying the same space of the chlorothiophene P1 moiety.

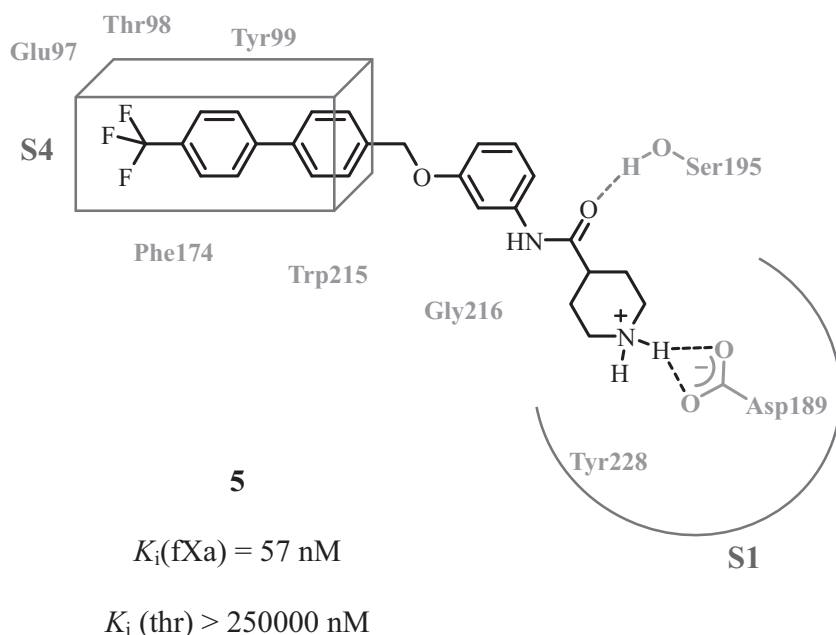


**Fig. 2.** Schematic representation of the binding mode of the highly potent and selective fXa inhibitor **5**, built up on the benzyloxyphenyl piperidine-4-carboxamide scaffold (de Candia et al., 2009b), into the binding site of fXa; S1 and S4 pockets and several residues important for ligand binding are depicted. The inhibition constant values ( $K_i$ ) against factor Xa and thrombin of compound **5**, which proved to be also a moderate inhibitor ( $\text{IC}_{50} = 65.7 \mu\text{M}$ ) of ADP-induced platelet aggregation, are shown.

Rivaroxaban **3** (Roehrig et al., 2005), apixaban **4** (Pinto et al., 2007) and other orally administered selective fXa inhibitors (Haginoya et al., 2004) have progressed to advanced phases of clinical studies (de Candia et al., 2009a).

In our previous work, we described new benzyloxy isonipecotanilide derivatives with dual function against thrombosis. In particular, the 4- $\text{CF}_3$  derivative of *N*-[3-(1,1'-biphenyl-4-ylmethoxy)phenyl]piperidine-4-carboxamide (**5**, Fig. 2) proved to be a potent and selective fXa inhibitor ( $K_i = 57 \text{ nM}$ ), showing additional antiplatelet effects with inhibition potency in the micromolar range (de Candia et al., 2009b).

Docking calculations suggested that compound **5** and its analogs bound human fXa through two main interactions: (i) salt bridge, strengthened by H-bonds, between the piperidinium group and the carboxylate of Asp189 at the bottom of the S1 subsite and (ii) H-bond between the amide carbonyl of the ligand/s and the catalytic residue Ser195. The consistent values of docking scores highlighted the relevant role played by hydrophobic interactions occurring between the distal phenyl group and the S4 aromatic pocket, reinforced by two middle-range contacts between  $\text{C}(\text{sp}^3)\text{-F}$  and CO moieties of Thr98 and Glu97.

Albeit interesting as *in vitro* fXa inhibitor and antiplatelet agent, compound **5** was too lipophilic. Its  $\log P$  (ca. 6) far exceeded the value of 4, which is suggested as the maximum calculated threshold for any fXa direct inhibitor that possesses good pharmacokinetics and *in vivo* anticoagulant activity (Remko, 2009). As a general trend, compounds with comparable binding affinity show better anticoagulant activity if their lipophilicity is lower.

With the aim of improving either anticoagulant activity or physicochemical profile of the biphenylmethoxy isonipecotanilide derivatives, we designed and synthesized new analogs, exploring less lipophilic variants of the 1,1'-biphenyl moiety in compound **5**. Hence, one phenyl group of the biphenyl moiety was replaced by the isoxazolyl group, and the 4- $\text{CF}_3$ -phenyl (distal) group with 4-Cl-phenyl and 2-Cl-thiophen-5-yl groups, which, as shown for a number of novel inhibitors (de Candia et al., 2009a; Pinto et al.,

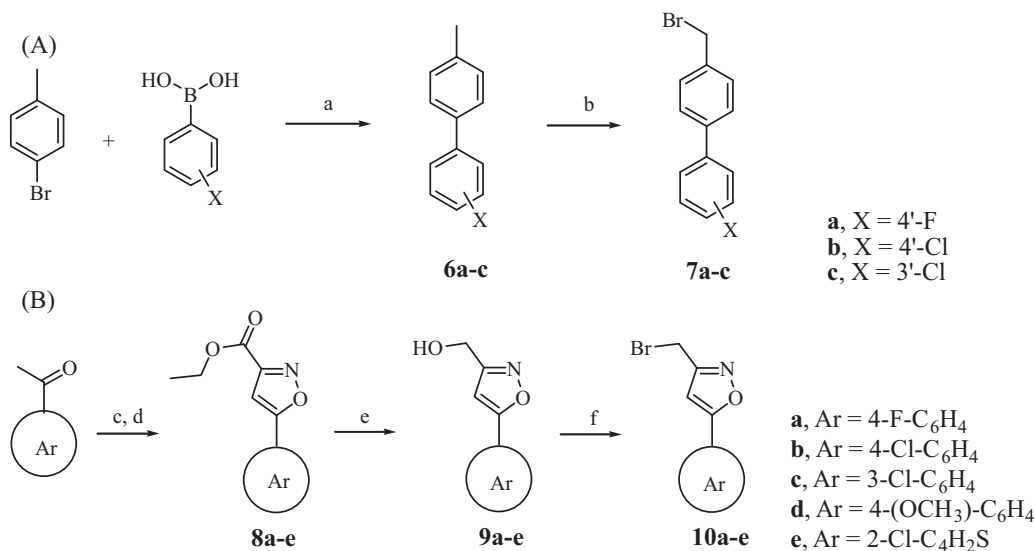
2010), may exploit the arylhalogen binding mode in the S1 pocket of fXa (Maignan et al., 2003). The effects on the activity of the basic amidine and isopropyl groups appended at the piperidine nitrogen (N1), as well as the *ortho*-substituted isomers of the biaryl methoxy derivatives, were also investigated.

Herein, we report synthesis, blood coagulation factors' enzyme inhibition, *in vitro* anticoagulant activity, structure–activity relationships (SARs) and molecular modeling of biaryl methoxy isonipecotanilide derivatives, highlighting the improvement in their fXa inhibition potency and selectivity, as well as in anticoagulant activity as assessed by clotting assays.

## 2. Materials and methods

Melting points were determined by using the capillary method on a Stuart Scientific SMP3 electrothermal apparatus and are not corrected. IR spectra were recorded using KBr disks on a Perkin-Elmer Spectrum One FT-IR spectrophotometer (Perkin-Elmer Ltd., Buckinghamshire, UK), and the most significant absorption bands expressed in  $\text{cm}^{-1}$  are listed.  $^1\text{H}$  NMR spectra were recorded at 300 MHz on a Varian Mercury 300 instrument. Chemical shift values are expressed in  $\delta$  and the coupling constants  $J$  in Hertz. Abbreviations are as follows: s, singlet; d, doublet; t, triplet; q, quartet; dd, doublet of doublets; m, multiplet; br, broad. Signals due to NH and OH protons were located by deuterium exchange with  $\text{D}_2\text{O}$ . Mass spectra were recorded on Agilent GC–MS 689–973. Elemental analyses (C, H, N) were performed on a Euro EA3000 analyzer (Eurovector, Milan, Italy) using the Analytical Laboratory Service of the Dipartimento Farmaco-Chimico of the University of Bari, and the results agreed to within 0.40% of the theoretical values. Chromatographic separations were performed on silica gel 60 for column chromatography (Merck 70–230 mesh, or alternatively 15–40 mesh for flash chromatography).

Several compounds were synthesized according to known procedures with slight modifications; their melting points and spectral data were in full agreement with those reported in literature, and no effort was made at this stage to optimize the yields. Unless



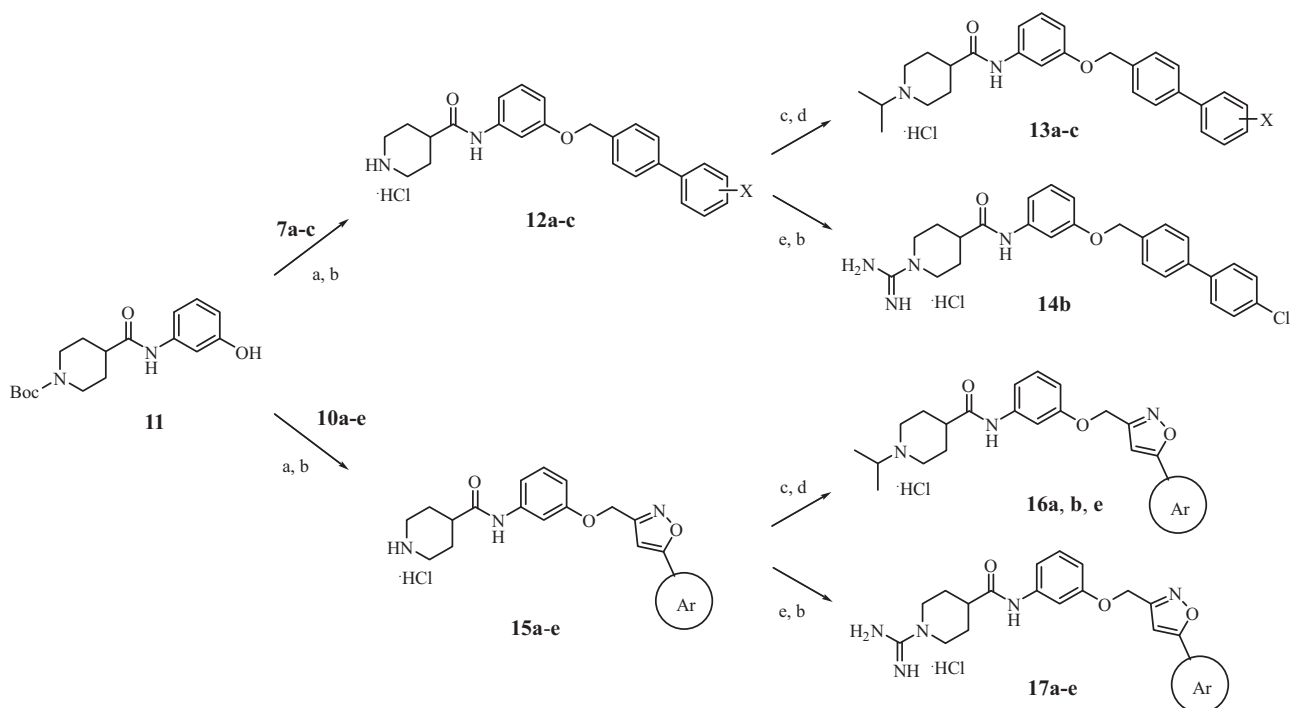
**Scheme 1.** Reagents and conditions: (a) K<sub>2</sub>CO<sub>3</sub>, TBAB (tetrabutylammonium bromide), Pd(OAc)<sub>2</sub>, PEG400, 110 °C, 16 h; (b) NBS (*N*-bromosuccinimide), AIBN (azobisisobutyronitrile), CCl<sub>4</sub>, reflux, 20 h; (c) *n*BuLi, dry THF, 0 °C, 10 min, then diethyloxalate, dry THF, rt, 3 h; (d) NH<sub>2</sub>OH·HCl, abs EtOH, reflux, 6 h; (e) NaBH<sub>4</sub>, abs. EtOH, dry THF, 0 °C, 4 h; (f) CBr<sub>4</sub>, PPh<sub>3</sub>, dry CH<sub>2</sub>Cl<sub>2</sub>, 4 h.

otherwise stated, all chemicals and solvents were purchased from Sigma–Aldrich.

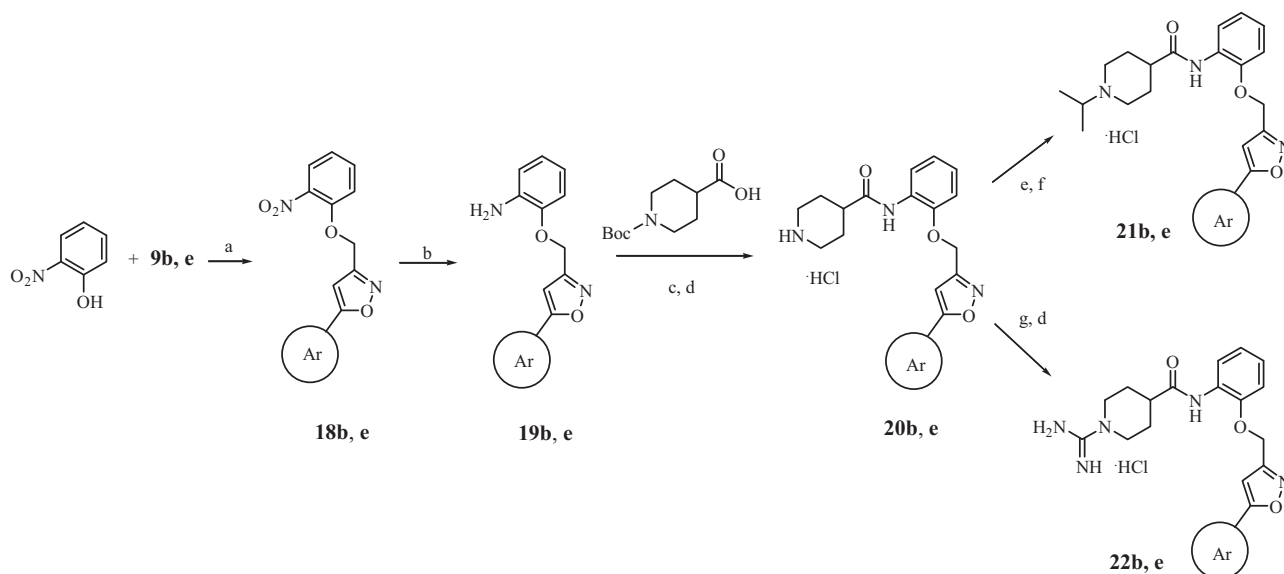
General synthesis procedures, along with physicochemical data, elemental analyses (C, H, N), IR and <sup>1</sup>H NMR spectra of some representative newly synthesized intermediates (**8a** and **10a**, Scheme 1; **18b** and **20b**, Scheme 3) and target compounds (**12b**, **13a** and **14b**, Scheme 2; **20b**, Scheme 3), are reported below. Characterization data for all the other newly synthesized compounds (**8b–e**, **12c**, **13b**, **13c**, **15a**, **15b**, **15e**, **16a**, **16b**, **16e**, **17a–e**, **18e**, **19e**, **20e**, **21b**, **21e**, **22b**, **22e**) are reported in Supporting Information available on the journal website.

### 2.1. General procedure for the synthesis of *X*-substituted 4-(bromomethyl)-1,1'-biphenyls (**7a–c**)

Compounds **7a–c** were prepared in two steps. Using *X*-substituted (*X* = 4-F, 4-Cl and 3-Cl) phenylboronic acids and 4-bromotoluene as the starting materials, a Suzuki cross-coupling reaction was carried out through a reported green chemistry procedure (Liu et al., 2006), that allowed the intermediate biphenyl derivatives **6a–c** to be obtained in high yields (>90%). The spectral data of **6a** (de Candia et al., 2009a,b), **6b** and **6c** (Miguez et al., 2007) were in full agreement with those already reported. In the



**Scheme 2.** Reagents and conditions: (a) NaH, dry DMF, rt, 4 h; (b) HCl gas, CHCl<sub>3</sub>, 0 °C, 30 min; (c) acetone, Na(CN)BH<sub>3</sub>, MeOH, rt, 24 h; (d) HCl (1.25 M) in MeOH, 0 °C, 30 min; (e) 1,3-bis(*tert*-butoxycarbonyl)-2-methyl-2-thioisourea, HgCl<sub>2</sub>, dry DMF, 0 °C to rt, 24 h.



**Scheme 3.** Reagents and conditions: (a) DIAD (diisopropylazodicarboxylate),  $\text{PPh}_3$ , dry THF, rt, 48 h; (b)  $\text{SnCl}_2 \cdot 2\text{H}_2\text{O}$ , DMF, rt, overnight; (c) DCC (dicyclohexylcarbodiimide), HOBT (1-hydroxybenzotriazole), dry THF, rt, 48 h; (d) HCl gas,  $\text{CHCl}_3$ ,  $0^\circ\text{C}$ , 30 min; (e) acetone,  $\text{Na}(\text{CN})\text{BH}_3$ , MeOH, rt, 24 h; (f) HCl (1.25 M) in MeOH,  $0^\circ\text{C}$ ; (g) 1,3-bis(*tert*-butoxycarbonyl)-2-methyl-2-thiopseudourea,  $\text{HgCl}_2$ , dry DMF,  $0^\circ\text{C}$  to rt, 24 h.

second step, to a solution of **6a** (or **6b** or **6c**) in  $\text{CCl}_4$ , a stoichiometric amount of *N*-bromosuccinimide (NBS) and a catalytic amount of azobisisobutyronitrile (AIBN) were added, and the reaction mixture was refluxed for 20 h. After cooling to room temperature, the insoluble succinimide was filtered off and the solvent was evaporated under reduced pressure to provide the target bromomethyl derivatives **7a–c** as crude yellow solids (yields in the 60–95% range, as assessed by GC–MS), which were used in the subsequent reactions without further purification. The spectral data of **7a** ( $X=4\text{'-F}$ ; de Candia et al., 2009b), **7b** ( $X=4\text{'-Cl}$ ; Van Duzer and Roland, 1994) and **7c** ( $X=3\text{'-Cl}$ ; Van Duzer and Roland, 1994) were in full agreement with the reported ones.

## 2.2. General procedure for the synthesis of ethyl 5-(aryl)isoxazole-3-carboxylates (**8a–e**)

Compounds **8a–e** were synthesized through known procedures (Nazaré et al., 2004, 2005), with slight modifications. The preparation of **8a** is described as representative example.

### 2.2.1. Ethyl 5-(4-fluorophenyl)isoxazole-3-carboxylate (**8a**)

To a stirred solution of 1-(4-fluorophenyl)ethanone (1.96 ml, 18.1 mmol) in 60 ml of dry THF, cooled at a  $0^\circ\text{C}$  and under argon atmosphere, a 2.5 M solution of *n*-butyl lithium in *n*-hexane (8.69 ml, 21.7 mmol) was added dropwise. After 10 min of stirring at  $0^\circ\text{C}$ , diethyl oxalate (2.95 ml, 21.7 mmol) was added dropwise, and stirring was continued at room temperature for 3 h. The reaction was then quenched by addition of aqueous 2 M HCl (13.6 ml, 27.1 mmol) and the mixture was partitioned between water and EtOAc. The aqueous phase was extracted twice with EtOAc and the combined organic layers were washed with brine, dried ( $\text{Na}_2\text{SO}_4$ ) and concentrated under reduced pressure to afford an oil residue. Hydroxylamine hydrochloride (1.38 g, 19.9 mmol) was added to the obtained residue dissolved in 50 ml of abs EtOH, and the mixture was refluxed for 6 h. After cooling to room temperature, the solvent was removed by evaporation under reduced pressure, and the obtained residue was dissolved in EtOAc and washed with water. The organic layer was dried ( $\text{Na}_2\text{SO}_4$ ) and concentrated under reduced pressure. Purification by silica gel chromatography of the residue, eluting with petroleum ether/EtOAc (90:10, v/v), provided

compound **8a** (1.85 g, 49% yield) as white solid, which was used in the subsequent reaction.

IR ( $\text{cm}^{-1}$ ) 1733, 1247, 1139, 842, 771, 812.  $^1\text{H}$  NMR ( $\text{CDCl}_3$ )  $\delta$  7.80 (dd, 2H,  $J=8.8, 5.2$  Hz), 7.19 (t, 2H,  $J=8.5$  Hz), 6.88 (s, 1H), 4.47 (q, 2H,  $J=7.2$  Hz), 1.44 (t, 3H,  $J=7.2$  Hz).

## 2.3. General procedure for the synthesis of 3-(bromomethyl)-5-arylisoxazoles (**10a–e**)

According to Scheme 1(B), the ethyl carboxylates **8a–e** were converted by reaction with  $\text{NaBH}_4$  into the corresponding methyl alcohols **9a–e** (yields in the range 85–95%), which were used in the subsequent bromination reaction without further purification. All the crude [5-arylisoxazol-3-yl]methanol products (**9a–e**) were converted to the corresponding 3-(bromomethyl)-5-arylisoxazole derivatives (**10a–e**) under mild conditions through the Appel reaction (Appel, 1975), using  $\text{CBr}_4$  and triphenylphosphine ( $\text{PPh}_3$ ), with good yields (60–95%, as assessed by GC–MS). The preparation of 3-(bromomethyl)-5-(4-fluorophenyl)isoxazole **10a** is reported as an example.

### 2.3.1. 3-(Bromomethyl)-5-(4-fluorophenyl)isoxazole (**10a**)

To a cooled solution of ethyl 5-(4-fluorophenyl)isoxazole-3-carboxylate **8a** (0.50 g, 2.13 mmol) in a mixture of 6 ml of dry THF and 6 ml of absolute ethanol,  $\text{NaBH}_4$  (0.12 g, 3.19 mmol) was added portionwise. The reaction mixture was stirred at  $0^\circ\text{C}$  for 4 h, then quenched by addition of aqueous 1 N HCl, and partitioned between EtOAc and water. The aqueous phase was twice extracted with EtOAc, and the combined organic layers were washed with brine, dried ( $\text{Na}_2\text{SO}_4$ ) and concentrated under reduced pressure to provide **9a** as white solid (0.35 g, 85% yield). To a solution of the product **9a** (0.35 g, 1.81 mmol) in 15 ml of  $\text{CH}_2\text{Cl}_2$  cooled at  $0^\circ\text{C}$ ,  $\text{CBr}_4$  (0.66 g, 1.99 mmol) and  $\text{PPh}_3$  (0.52 g, 1.99 mmol) were added, and the mixture was stirred at room temperature for 24 h. After the removal of the solvent under reduced pressure, the residue was purified by silica gel chromatography, using the petroleum ether/EtOAc mixture (90:10, v/v), and compound **10a** obtained as pale brown solid (0.29 g, 62% yield).

## 2.4. General procedure for the synthesis of compounds **12a–e** and **15a–e**

The piperidine-4-carboxamides derivatives **12a–e** and **15a–e** were synthesized according to previously reported procedures (de Candia et al., 2009a,b). The preparation of compound **12b** as HCl salt is reported as an example.

### 2.4.1. *N*-{3-[(4'-Chloro-1,1'-biphenyl-4-yl)methoxy]phenyl}piperidine-4-carboxamide hydrochloride (**12b**)

A solution of *t*-butyl 4-[*N*-(3-hydroxyphenyl)carbamoyl]piperidine-1-carboxylate **11** (1.56 g, 4.86 mmol) in 5 ml of dry DMF was added to a suspension of NaH (0.14 g, 5.83 mmol) in 6 ml of dry DMF at room temperature. After 15 min of stirring, a solution of 4-(bromomethyl)-4'-chloro-1,1'-biphenyl (1.37 g, 4.86 mmol) in 6 ml of dry DMF was added dropwise. The reaction mixture was stirred for 4 h at room temperature, and then quenched by adding 5 ml of 5% (w/v) KHSO<sub>4</sub>. The mixture was then diluted with water and extracted with EtOAc. The combined organic extracts were washed with 2 N NaOH, brine, dried (Na<sub>2</sub>SO<sub>4</sub>) and concentrated under reduced pressure. The residue was purified by silica gel chromatography, eluting with petroleum ether/EtOAc (90:10, v/v), and the chromatographically pure *N*-BOC protected derivative was treated in chloroform solution with HCl gas to remove the BOC protecting group. Subsequent purification by crystallization afforded **12b** as white solid (1.45 g, 65% yield), mp 246–248 °C from EtOH/EtOAc. IR (cm<sup>-1</sup>) 3142, 2955, 1661, 1226, 1160, 1137, 1091, 1036, 809, 779. <sup>1</sup>H NMR (DMSO-*d*<sub>6</sub>) δ 10.11 (s, 1H), 8.72 (br, 2H), 7.70–7.66 (m, 4H), 7.58–7.49 (m, 4H), 7.42 (s, 1H), 7.21–7.11 (m, 2H), 6.70 (d, 1H, *J* = 7.7 Hz), 5.10 (s, 2H), 3.29 (d, 2H, *J* = 13.2 Hz), 2.89 (d, 1H, *J* = 12.4 Hz), 2.85 (d, 1H, *J* = 12.4 Hz), 2.65–2.58 (m, 1H), 1.97–1.94 (m, 2H) and 1.90–1.72 (m, 2H). MS (ESI, positive ion) *m/z*: 421.1 (M+H). Anal. Calcd. for C<sub>25</sub>H<sub>25</sub>ClN<sub>2</sub>O<sub>2</sub> × HCl × H<sub>2</sub>O: C, 63.16; H, 5.94; N, 5.89%; found: C, 63.55; H, 5.69; N, 6.03%.

### 2.5. General procedure for the synthesis of 1-isopropylpiperidine-4-carboxamide derivatives (**13a–c**, **16a, b**, **e** and **21b, e**)

The introduction of the isopropyl group on piperidine nitrogen was achieved by one pot reductive alkylation of the piperidine-4-carboxamide derivatives (yields: 38–95%). The preparation of *N*-{3-[(4'-chloro-1,1'-biphenyl-4-yl)methoxy]phenyl}piperidine-4-carboxamide hydrochloride **13a** is reported as an example.

### 2.5.1. *N*-{3-[(4'-Fluoro-1,1'-biphenyl-4-yl)methoxy]phenyl}-1-(1-methylethyl)piperidine-4-carboxamide hydrochloride (**13a**)

To a cooled solution of the already reported *N*-{3-[(4'-fluoro-1,1'-biphenyl-4-yl)methoxy]phenyl}piperidine-4-carboxamide hydrochloride (de Candia et al., 2009a,b) **12a** (0.33 g, 0.76 mmol) in 15 ml of MeOH, acetone (2 ml) and Na(CN)BH<sub>3</sub> (52 mg, 0.83 mmol) were added. The reaction mixture was stirred at room temperature for 24 h, and then concentrated under reduced pressure. The residue was partitioned between EtOAc and 2 N NaOH, and the aqueous layer was separated and extracted twice with EtOAc. The combined organic layers were dried (Na<sub>2</sub>SO<sub>4</sub>) and concentrated under reduced pressure to afford the free base, which was converted into the hydrochloride salt by treatment with 5 ml of 1 N HCl in MeOH at 0 °C for 30 min. Removal of the solvent in vacuo and purification by crystallization afforded the 0.16 g (44% yield) of the product HCl salt **13a** as white microcrystalline solid; mp 223–225 °C, from EtOH/EtOAc. IR (cm<sup>-1</sup>) 3137, 1669, 1224, 1158, 1035, 811, 775, 688. <sup>1</sup>H NMR (DMSO-*d*<sub>6</sub>) δ 10.14 (s, 1H), 9.73 (br,

1H), 7.70 (dd, 2H, *J* = 9.3, 5.2 Hz), 7.66 (d, 2H, *J* = 8.3 Hz), 7.50 (d, 2H, *J* = 8.2 Hz), 7.43 (s, 1H), 7.28 (t, 2H, *J* = 8.8 Hz), 7.22–7.12 (m, 2H), 6.71 (d, 1H, *J* = 7.4 Hz), 5.10 (s, 2H), 3.43 (d, 2H, *J* = 10.5 Hz), 3.25–3.21 (m, 1H), 2.92–2.83 (m, 2H), 2.64–2.55 (m, 1H), 2.08–1.89 (m, 4H) and 1.26 (d, 6H, *J* = 6.6 Hz). MS (ESI, positive ion) *m/z*: 447.1 (M+H). Anal. Calcd. for C<sub>28</sub>H<sub>31</sub>ClN<sub>2</sub>O<sub>2</sub> × HCl × 2.5H<sub>2</sub>O: C, 61.71; H, 6.80; N, 5.14%; found: C, 61.54; H, 6.45; N, 5.28%.

### 2.6. General procedure for guanylation of compounds **12b** (**14b**), **15a–e** (**17a–e**) and **20b, e** (**22b, e**)

The preparation of *N*-{3-[(4'-chloro-1,1'-biphenyl-4-yl)methoxy]phenyl}-1-carbamimidoylpiperidine-4-carboxamide hydrochloride **14b** is reported as a representative example.

### 2.6.1. *N*-{3-[(4'-Chloro-1,1'-biphenyl-4-yl)methoxy]phenyl}-1-carbamimidoylpiperidine-4-carboxamide hydrochloride (**14b**)

1,3-bis(tertbutoxycarbonyl)-2-methyl-2-thiopseudourea (0.38 g, 1.31 mmol), mercury(II) chloride (0.36 g, 1.31 mmol) and triethylamine (0.46 ml, 3.27 mmol) were added to a cooled solution (0 °C) of *N*-{3-[(4'-chloro-1,1'-biphenyl-4-yl)methoxy]phenyl}piperidine-4-carboxamide hydrochloride **12b** (0.50 g, 1.09 mmol) in 8 ml of dry DMF. The reaction mixture was stirred for 1 h at 0 °C and 24 h at room temperature; 10 ml of EtOAc were then added, and stirring was continued for 15 min. The precipitate was filtered off and washed 3 times with EtOAc. The combined organic phases were washed with brine, dried (Na<sub>2</sub>SO<sub>4</sub>), and concentrated under reduced pressure to afford a residue, which was purified by silica gel chromatography, eluting with petroleum ether/EtOAc (90:10, v/v). The pure *N,N'*-bis-BOC protected derivative obtained was treated with HCl gas in chloroform solution to afford 0.21 g (39% yield) of the product HCl salt **14b** as white microcrystalline solid; mp 260–261 °C, from EtOH/EtOAc. IR (cm<sup>-1</sup>) 3211, 1651, 1222, 1156, 1093, 1038, 954, 872, 810, 774. <sup>1</sup>H NMR (DMSO-*d*<sub>6</sub>) δ 10.06 (s, 1H), 7.77–7.66 (m, 4H), 7.58–7.48 (m, 4H), 7.44 (br, 4H), 7.21–7.12 (m, 2H), 6.70 (d, 1H, *J* = 8.0 Hz), 5.10 (s, 2H), 3.88 (d, 2H, *J* = 13.6 Hz), 3.06 (d, 1H, *J* = 12.1 Hz), 3.02 (d, 1H, *J* = 11.3 Hz), 2.68–2.61 (m, 1H), 1.88–1.83 (m, 2H) and 1.64–1.52 (m, 2H). MS (ESI, positive ion) *m/z*: 463.1 (M+H). Anal. Calcd. for C<sub>27</sub>H<sub>26</sub>ClN<sub>3</sub>O<sub>2</sub> × HCl × H<sub>2</sub>O: C, 60.35; H, 5.84; N, 10.83%; found C, 60.74; H, 5.65; N, 11.07%.

### 2.7. General procedure for the synthesis of 2-[(5-arylisoxazol-3-yl)methoxy]aniline derivatives (**19b, e**)

The aniline derivatives **19b** and **19e**, necessary for synthesizing the *ortho* isomers of the biaryl-containing piperidine-4-carboxamides **20b** and **20e** (Scheme 3), were prepared in two steps. At first, a Mitsunobu coupling was carried out with 2-nitrophenol and suitable 5-arylisoxazol-3-yl-methanol derivatives **9b** and **9e**, to furnish the nitrophenyl compounds **18b** and **18e**, which were then reduced to **19b** and **19e** using SnCl<sub>2</sub> × 2H<sub>2</sub>O. The preparation of compound **19b** is reported as an example.

### 2.7.1. 5-(4-Chlorophenyl)-3-[(2-nitrophenoxy)methyl]isoxazole (**18b**)

To a cooled (0 °C) stirred solution of 2-nitrophenol (1.15 g, 8.28 mmol), PPh<sub>3</sub> (2.17 g, 8.28 mmol), and [5-(4-chlorophenyl)isoxazol-3-yl]methanol **9b** (1.74 g, 8.28 mmol) in 20 ml of dry THF, diisopropylazodicarboxylate DIAD (1.63 ml, 8.28 mmol), dissolved in 5 ml of dry THF, was added dropwise, and the mixture was stirred at room temperature for about 48 h. After removal of the solvent under reduced pressure, the oil residue was purified by silica gel chromatography, eluting with petroleum

ether/EtOAc (90:10, v/v), to provide compound **18b** (1.65 g, 60% yield) as pale-yellow solid. IR ( $\text{cm}^{-1}$ ) 1615, 1529, 1347, 1277, 1257, 1094, 1003, 864, 835, 799, 740.  $^1\text{H}$  NMR ( $\text{CDCl}_3$ )  $\delta$  7.88 (d, 1H,  $J=8.3$  Hz), 7.74 (d, 2H,  $J=6.6$  Hz), 7.55 (t, 1H,  $J=8.8$  Hz), 7.45 (d, 2H,  $J=6.6$  Hz), 7.23 (d, 1H,  $J=8.0$  Hz), 7.10 (t, 1H,  $J=8.3$  Hz), 6.74 (s, 1H) and 5.35 (s, 2H).

### 2.7.2. 2- $\{[5-(4\text{-Chlorophenyl})\text{isoxazol-3-yl}]\text{methoxy}\}$ aniline (**19b**)

$\text{SnCl}_2 \times 2\text{H}_2\text{O}$  (6.19 g, 27.4 mmol) was added to a solution of **18b** (1.65 g, 5.49 mmol) in 15 ml of DMF. The reaction mixture was stirred overnight at room temperature, and then poured into ice and alcalinized to pH 12 by adding aqueous 2 N NaOH. The resulting suspension was filtered, and the collected solid was washed with  $\text{Et}_2\text{O}$ . The aqueous phase was extracted twice with  $\text{Et}_2\text{O}$ , and the combined organic phases were washed with brine, dried ( $\text{Na}_2\text{SO}_4$ ), and concentrated under reduced pressure. The oil residue was purified by silica gel chromatography, eluting with petroleum ether/EtOAc (60:40, v/v), to yield 0.99 g of the product **19b** (60%) as pale-red solid.

IR ( $\text{cm}^{-1}$ ) 3442, 3358, 1613, 1508, 1460, 1435, 1280, 1217, 1095, 1055, 835, 818, 734.  $^1\text{H}$  NMR ( $\text{CDCl}_3$ )  $\delta$  7.72 (d, 2H,  $J=9.1$  Hz), 7.44 (d, 2H,  $J=9.1$  Hz), 6.92–6.82 (m, 2H), 6.77–6.70 (m, 2H), 6.63 (s, 1H), 5.22 (s, 2H), 3.83 (br, 2H).

## 2.8. General procedure for the synthesis of substituted *N*-(2- $\{[5\text{-aryl}]\text{isoxazol-3-yl}]\text{methoxy}\}$ phenyl)piperidine-4-carboxamides hydrochloride (**20b, e**)

The preparation of compound **20b** is reported as an example.

### 2.8.1. *N*-(2- $\{[5-(4\text{-Chlorophenyl})\text{isoxazol-3-yl}]\text{methoxy}\}$ phenyl)piperidine-4-carboxamide hydrochloride (**20b**)

*N*-Hydroxybenzotriazole hydrate (0.44 g, 3.28 mmol), *N,N'*-dicyclohexylcarbodiimide (0.68 g, 3.28 mmol) were added to a cooled solution of 1-(*t*-butoxycarbonyl)piperidine-4-carboxylic acid (0.82 g, 3.61 mmol) in 15 ml of THF. After stirring for 30 min, 2- $\{[5-(4\text{-chlorophenyl})\text{isoxazol-3-yl}]\text{methoxy}\}$ aniline **19b** (0.99 g, 3.28 mmol) was added, and the reaction mixture was stirred at room temperature for 48 h. Then, the formed dicyclohexylurea was filtered off and the filtrate was concentrated under reduced pressure. The obtained residue was dissolved in EtOAc and sequentially washed with 5% (w/v)  $\text{NaHCO}_3$ , 1 N HCl and brine. The organic phase was dried ( $\text{Na}_2\text{SO}_4$ ) and concentrated under reduced pressure, to provide the *N*-BOC protected derivative, which was treated with HCl gas in chloroform solution for removing the BOC protecting group. Purification by crystallization of the crude product afforded 0.80 g of compound **20b** (50% yield) as white microcrystalline solid; mp 211–215 °C from EtOH/EtOAc. IR ( $\text{cm}^{-1}$ ): 3129, 1664, 1205, 1092, 1052, 800, 766, 754.  $^1\text{H}$  NMR ( $\text{DMSO-}d_6$ )  $\delta$  9.22 (s, 1H), 8.84 (br, 1H), 8.67 (br, 1H), 7.88 (d, 2H,  $J=9.1$  Hz), 7.78 (d, 1H,  $J=7.3$  Hz), 7.61 (d, 2H,  $J=8.5$  Hz), 7.23 (s, 1H), 7.18 (d, 1H,  $J=7.3$  Hz), 7.09 (t, 1H,  $J=7.0$  Hz), 6.94 (t, 1H,  $J=7.0$  Hz), 5.29 (s, 2H), 3.25 (d, 2H,  $J=12.4$  Hz), 2.90–2.75 (m, 3H) and 1.94–1.73 (m, 4H). MS (ESI, positive ion)  $m/z$ : 412.0 (M+H). Anal. Calcd. for  $\text{C}_{22}\text{H}_{22}\text{ClN}_3\text{O}_3 \times \text{HCl} \times \text{H}_2\text{O}$ : C, 56.66; H, 5.40; N, 9.01%; found: C, 56.27; H, 5.30; N, 8.71%.

## 2.9. Inhibition assays of factor Xa and related serine proteases

The target compounds were assessed for their inhibitory activity toward factor Xa (fXa), thrombin, and  $\alpha$ -chymotrypsin ( $\alpha$ -CT) by kinetic analysis using chromogenic substrates monitored at 405 nm. All buffer salts were obtained from Sigma–Aldrich Co.

(Milan, Italy). Enzymes and substrates were obtained as follows: for fXa kinetic studies, 2 nM human factor Xa and 0.04 mM S-2765 (Z-D-Arg–Gly–Arg-*p*-nitroanilide) from Chromogenix AB-Instrumentation Laboratories (Milan, Italy); for fIIa kinetic studies, 0.41 U/ml bovine thrombin from Sigma–Aldrich (Milan, Italy) and 0.050 mM S-2238 (D-Phe–Pip–Arg-*p*-nitroanilide) from Chromogenix AB-Instrumentation Laboratories (Milan, Italy); for  $\alpha$ -CT kinetic studies, 0.4  $\mu\text{g}/\text{ml}$  bovine  $\alpha$ -chymotrypsin and 0.185 mM *N*-succinyl–Ala–Ala–Pro–Phe-*p*-nitroanilide from Sigma–Aldrich Co. (Milan, Italy). In kinetic studies with fXa or thrombin, 500  $\mu\text{l}$  of the enzyme solution in a 10 mM Tris buffer (pH 8), containing 0.15 M NaCl and 0.1% of PEG 6000, was mixed with 10  $\mu\text{l}$  of DMSO solution of the test compound, its final concentration ranging from 100  $\mu\text{M}$  to 0.1 nM; DMSO, derived from stock solutions, did not exceed a final concentration of 1% (v/v) (10  $\mu\text{l}$  of DMSO in control assays). The enzymes were incubated with the test compound or its solvent (DMSO) for 30 min at 25 °C, and the reactions were initiated by the addition of 500  $\mu\text{l}$  of the appropriate substrate solution in buffer. Increase in absorbance due to proteolytic cleavage of the substrate was monitored at 25 °C and 405 nm for 5 min.

In kinetic studies with  $\alpha$ -CT, 845  $\mu\text{l}$  of 50 mM Tris buffer (pH 7.5), containing 50 mM of  $\text{CaCl}_2$ , were added to 50  $\mu\text{l}$  of enzyme solution in buffer and 5  $\mu\text{l}$  of solution of the test compound (final concentration ranging from 10 nM to 0.25 mM) or its solvent. After 10 min of incubation at 25 °C, 100  $\mu\text{l}$  of the substrate solution in buffer was added and the absorbance increase at 405 nm was monitored at 25 °C for 5 min. Initial velocities were determined by analysis of the initial linear portion of the kinetic curve, and values were plotted against log inhibitor concentration.  $\text{IC}_{50}$  values were obtained by nonlinear (sigmoid) regression calculation on dose–response plots in at least three different determinations, and used in the Cheng–Prusoff equation for calculating inhibition constants  $K_i$  (Cheng and Prusoff, 1973).

## 2.10. *In vitro* coagulation assays

Pooled lyophilized human plasma (100  $\mu\text{l}$ ) and PT reagent (200  $\mu\text{l}$ ) (Futura System s.r.l., Formello, Rome, Italy) were used. Inhibitor or solvent (DMSO, max 1%, v/v) was added to plasma and incubated for 3 min at 37 °C. Clotting times (s) were determined in a coagulometer (Behnk electronic GmbH, Norderstedt, Germany) and compared with those from the appropriate human control plasma. Each measurement was performed in triplicate, and the concentrations of the test compound which caused a 2-fold prolongation of the prothrombin time ( $\text{PT}_2$ ) were calculated from concentration–response curves.

## 2.11. Determination of lipophilicity parameters by hydrophilic interaction liquid chromatography (HILIC)

Retention measurements were performed at 23 °C by using a ZIC-*p*HILIC column (sulfoalkylbetaine phase on a polymeric support, 10 cm  $\times$  4.6 mm, 5  $\mu\text{m}$ ) from SeQuant (Umeå, Sweden). All the measurements were made at temperature of 23 °C, flow-rate 1.0 ml/min on a Merck Hitachi EliteLaChrom liquid chromatograph (Merck, Darmstadt, Germany, and Hitachi Instrument, Inc., San Jose, CA, USA) equipped with a L-2200 auto sampler, a L-2130 pump, and a L-7614 degasser. Detection was performed using a L-2400 UV detector operating at 230 nm for all the analyzed compounds. The chromatographic system was controlled by a EzChrom Elite System Manager software version 3.1.7.

Phoebus software 1.0 (Sedere, Centre Analyze, Orleans, France) was used to prepare buffer (trifluoroacetic acid/ammonium) at pH 2 and ionic strength (*I*) equal to 100 mM. The pH of the mobile phase were measured both before ( $^w\text{pH}$ ) and after the adjunction

**Table 1**

Inhibition constants for fXa and thrombin (thr) of 1,1'-biphenylmethoxy isonipecotanilides **12–14**.

No.	X	$K_i$ (nM) <sup>a</sup>		$\log P_{\text{calc}}^b$
		fXa	thr	
<b>12a</b>	4'-F	3870 <sup>c</sup>	c,d	5.14
<b>12b</b>	4'-Cl	33300	d	5.58
<b>12c</b>	3'-Cl	3215	d	5.58
<b>13a</b>	4'-F	139	d	6.25
<b>13b</b>	4'-Cl	165	d	6.70
<b>13c</b>	3'-Cl	16630	20730	6.70
<b>14b</b>	4'-Cl	31	2040	4.80

<sup>a</sup> In vitro inhibition constants against human fXa and bovine thr. Data are means of at least three different determinations, each performed in duplicate (S.E.M. < 5% of the mean).

<sup>b</sup> Log of 1-octanol/water partition coefficient calculated using KOWWIN v. 1.67 program (USEPA, 2007) within the EPI Suite™s.

<sup>c</sup> Previously reported data (de Candia et al., 2009a,b).

<sup>d</sup> Less than 30% inhibition at the maximum concentration tested (100 μM).

of organic solvent (<sup>s</sup><sub>w</sub>pH), with the pH-meter calibrated in aqueous buffer in both cases, even if <sup>s</sup><sub>w</sub>pH values have to be taken carefully (Roses and Bosch, 2002).

According to Bard et al. (2009) and Guillot (2010), the difference parameter ( $\Delta \log k_{0-95}$ ) between two isocratic log *k* values of the basic compounds in their cationic forms, namely log *k*<sub>0</sub>, that is the log *k* obtained in 100% aqueous buffer (pH 2) mobile phase, and log *k*<sub>95</sub>, that is the isocratic log *k* measured using a 95% (v/v) ACN–aqueous buffer (pH 2) mobile phase, allows the partition coefficient of their neutral form (log *P*<sup>N</sup>) to be determined. The HILIC log *k* values are summarized in a table reported in Supporting Information. This method offers fast measurements of lipophilicity parameters for lipophilic strong basic compounds (Eq. (1); Bard et al., 2009):

$$\log P^N = 1.07(\pm 0.056) \Delta \log k_{0-95} + 0.61(\pm 0.162)$$

$$n = 44; r^2 = 0.957; s = 0.39; F = 9353 \quad (1)$$

The experimental values demonstrated that these strong basic compounds remain lipophilic in their neutral form (4.12 < log *P*<sup>N</sup> < 5.46) but also suggested distribution coefficients at pH 7.4 (1.57 < log *D* < 3.01) adequate for good pharmacokinetic properties. The comparison between the lipophilicity parameters obtained by HILIC and those calculated using KOWWIN v. 1.67 program (USEPA, 2007) within the EPI Suite™s (Tables 2 and 3) confirm that compounds **15**, **16**, **17**, **20**, **21** and **22** are less lipophilic than compounds **12**, **13** and **14** (Table 1). The differences between calculated and experimental log *P* may result mostly from the theoretical method used for compounds **15**, **16**, **20** and **21**. For guanidine derivatives **17** and **22** the larger differences may also reflect the particular retention mechanism on HILIC phases (plot in Supporting Information). Work, out of the scope of this study, is in progress to clarify this point.

## 2.12. Molecular docking calculations

Unlike our previous simulations (de Candia et al., 2009b) performed with the program QXP (McMartin and Bohacek, 1997), the software GOLD (Jones et al., 1997) was herein preferred for docking analysis because it was extensively trained on a large number of complexes selected from the CCDC/ASTEX validation set including a large number of crystal structures of serine proteases (Nissink et al., 2002). GOLD is equipped with two equally reliable fitness functions, namely ChemScore and GoldScore (Verdonk et al., 2003), the latter being the first and most widely used and thus

**Table 2**

Inhibition constants for fXa, thrombin (thr), α-chymotrypsin (α-CT), and anti-coagulant activity of the meta-substituted isoxazole-containing biaryl methoxy isonipecotanilides **15–17**.

No.	Ar	$K_i^a$ (nM)			PT <sub>2</sub> <sup>b</sup> (μM)	log <i>P</i> <sup>N</sup> <sup>c</sup>	log <i>P</i> <sub>calc</sub> <sup>d</sup>
		fXa	thr	α-CT			
<b>15a</b>	4-F-phenyl	50000	e	e	ND	4.42	3.36
<b>15b</b>	4-Cl-phenyl	4680	e	e	307	4.72	3.80
<b>15e</b>	2-Cl-thiophen-5-yl	310	e	28200	327	4.64	3.62
<b>16a</b>	4-F-phenyl	2280	20100	e	282	5.21	4.48
<b>16b</b>	4-Cl-phenyl	218	e	21400	196	5.46	4.92
<b>16e</b>	2-Cl-thiophen-5-yl	95	16000	35400	71.3	5.44	4.74
<b>17a</b>	4-F-phenyl	447	18300	4240	>500	4.99	2.58
<b>17b</b>	4-Cl-phenyl	26	6340	59100	109	5.37	3.02
<b>17c</b>	3-Cl-phenyl	388	15380	1970	226	5.29	3.02
<b>17d</b>	4-(OCH <sub>3</sub> )-phenyl	127	16000	5490	124	4.92	2.46
<b>17e</b>	2-Cl-thiophen-5-yl	15	15000	5810	122	5.25	2.84

<sup>a</sup> In vitro inhibition constants against human fXa and bovine thr and α-CT. Data are means of at least three different determinations, each performed in duplicate (S.E.M. < 5% of the mean).

<sup>b</sup> Concentration required to double the prothrombin time in human plasma.

<sup>c</sup> 1-Octanol/water partition coefficient of neutral form calculated with Eq. (1) (Guillot, 2010) using the difference parameter ( $\Delta \log k_{0-95}$ ) between two isocratic log *k* values of the basic compounds in their cationic forms, as assessed by hydrophilic interaction liquid chromatography (HILIC; definitions and details in Section 2).

<sup>d</sup> Log of 1-octanol/water partition coefficient calculated using KOWWIN v. 1.67 program (USEPA, 2007) within the EPI Suite™s.

<sup>e</sup> Less than 30% inhibition at the maximum concentration tested (100 μM).

selected for our investigations. The GoldScore fitness function is based on a linear combination of values relative to protein–ligand hydrogen bond (HB), protein–ligand and ligand internal van der Waals forces and ligand torsional strain energies. The interested reader is referred elsewhere for an in-depth description of the GOLD docking principles (Jones et al., 1997; Verdonk et al., 2003).

The X-ray crystal structure of human fXa in complex with a 1*H*-indole-2-carboxamide-based inhibitor (PDB code: 2BOH) (Nazaré et al., 2005) was retrieved and used as the target structure. According to reported computational procedures used by us in ligand- and structure-based design of serine protease inhibitors (Nicolotti et al., 2008, 2009, 2010), GOLD settings were tuned and calibrated by docking the co-crystallized ligand (2BOH) within its empty crystal structures. Residues within a radius of 11 Å from the alpha carbon of Gly216 were considered in docking simulations. The inhibitor molecules were built using the Sybyl fragment libraries (Tripos Associates, St. Louis, MO, USA). Geometrical optimization and charge calculation were performed by means of a quantum mechanical method with the PM3 Hamiltonian. Conformational analysis and molecular overlays were performed according to the procedures and methods described previously. According to Murcia et al. (2006), the basic N1 amino and amidine groups of the ligands were protonated, whereas the carboxylic groups in the protein residues were considered to be deprotonated. The target protein was prepared by removing water and the co-crystallized inhibitors. Controls were carefully carried out on the protonation state of polar residues leaning into the active site (Böhm et al., 1999). Using the 'Protein Preparation' module in Maestro 7.5 (Maestro 7.5.112; Schrödinger, LLC: New York), light relaxation was performed to optimise hydroxyl and thiol torsions followed by all-atom constrained minimization to relieve steric clashes until the RMSD reached 0.18 Å. Using the refined crystal structures, GOLD was set to generate 10 docking poses per run for each calculated ligand.

**Table 3**  
Inhibition constants for fXa, thrombin (thr),  $\alpha$ -CT, and anticoagulant activity of the *ortho*-substituted biarylmethoxy isonipecotanilides **20–22**.

No.	Ar	$K_i^a$ (nM)			PT <sub>2</sub> <sup>b</sup> ( $\mu$ M)	log P <sup>N</sup> <sup>c</sup>	log P <sub>calc</sub> <sup>d</sup>
		fXa	thr	$\alpha$ -CT			
<b>20b</b>	4-Cl-phenyl	11740	<sup>e</sup>	<sup>e</sup>	390	4.40	3.24
<b>20e</b>	2-Cl-thiophen-5-yl	54	<sup>e</sup>	<sup>e</sup>	190	4.12	3.06
<b>21b</b>	4-Cl-phenyl	7	13700	53900	13.3	5.19	4.36
<b>21e</b>	2-Cl-thiophen-5-yl	0.3	11010	60000	3.30	5.03	4.18
<b>22b</b>	4-Cl-phenyl	60	21200	34700	52.8	4.96	2.46
<b>22e</b>	2-Cl-thiophen-5-yl	2	6824	<sup>e</sup>	10.6	4.78	2.28

<sup>a–e</sup>: See footnotes to Table 2.

### 3. Results and discussion

#### 3.1. Chemistry

The isonipecotamide-based derivatives investigated in this study (**12–17** and **20–22**) were synthesized as shown in Schemes 1–3.

The 4-(bromomethyl)-1,1'-biphenyl intermediates **7a–c** were prepared in good yields according to Scheme 1(A). A Suzuki cross-coupling reaction was performed through a cheap green-chemistry procedure (Liu et al., 2006), using PEG400 as the solvent and very low amounts of palladium acetate as catalyst, which afforded the biphenyl derivatives **6a–c** in high yields. Subsequent radical bromination of compounds **6a–c** yielded the target bromides **7a–c**. The 3-(bromomethyl)-5-arylisoxazole intermediates **10a–e** were prepared according to the reaction pathway illustrated in Scheme 1(B). The ethyl 5-arylisoxazol-3-carboxylate derivatives **8a–e** were accessed, using slight modifications of known procedures (Nazaré et al., 2005), through lithiation of 1-arylethanones, carried out in dry THF at 0 °C, and subsequent reaction of the generated carbanions with diethyl oxalate. The obtained dicarbonyl intermediates were treated with hydroxylamine hydrochloride to afford compounds **8a–e**, which were then reduced to primary alcohols **9a–e** with NaBH<sub>4</sub>. Their bromination with CBr<sub>4</sub> and PPh<sub>3</sub> yielded the target derivatives **10a–e**.

The *meta*-substituted isonipecotanilides **12–17** were synthesized as shown in Scheme 2. The *N*-BOC protected phenol intermediate **11** (de Candia et al., 2009a,b) was alkylated with the bromomethyl-biaryl derivatives **7a–c** and **10a–e**. Removal of the BOC-protecting group by treatment with HCl gas afforded the desired products **12a–c** and **15a, b, e** as hydrochloride salts. Their reductive amination with acetone afforded *N*-isopropyl isonipecotanilides, which were then converted into the respective HCl salts **13a–c** and **16a, b, e**, whereas their reaction with 1,3-bis(tert-butoxycarbonyl)-2-methyl-2-thiopseudourea and HgCl<sub>2</sub> in dry DMF, followed by BOC deprotection, yielded the HCl salts of the guanidine derivatives **14b** and **17a–e**.

The *ortho*-substituted isonipecotanilides **20–22** were synthesized as shown in Scheme 3. Mitsunobu reaction (Mitsunobu, 1981) between 2-nitrophenol and (5-arylisoxazol-3-yl)methanol derivatives, using diethylazodicarboxylate (DIAD) and PPh<sub>3</sub>, yielded nitrophenylether derivatives **18b, e**, which were then reduced to **19b, e**. Coupling them with *N*-BOC-isonipecotic acid, followed by removal of the BOC-protecting group, yielded the target compounds **20b, e** as HCl salts, which were then converted to compounds **21b, e** and **22b, e**, using the afore-mentioned procedures.

#### 3.2. Structure–activity relationships

The newly synthesized isonipecotamide-based compounds, which are fully protonated under the condition of the biological assay at pH equal to 8, were evaluated in vitro for inhibition of fXa and thrombin and their potencies, expressed as inhibition constants ( $K_i$ , nM), are summarized in Tables 1–3. In addition, the *meta*- and *ortho*-substituted isoxazole-containing derivatives (**15–17** in Table 2 and **20–22** in Table 3, respectively) were assayed for their selectivity over  $\alpha$ -chymotrypsin ( $\alpha$ -CT), taken as a surrogate determination for achieving selectivity over other enzymes of the trypsin-like protease family for protein digestion in the gastrointestinal tract, and further characterized using the prothrombin time (PT) clotting assay in human plasma (the in vitro anticoagulant potency is reported as the concentration of inhibitor required to produce a doubling of the uninhibited clotting time, PT<sub>2</sub>).

The enzyme inhibition data of the 4(or 3)-halogen-1,1'-biphenyl-containing isonipecotanilide derivatives **12–14** (Table 1; previously reported data of compound **12a** are included for comparison) allowed us to expand the SAR scope of molecules encompassing compound **5** to N1-substitution with isopropyl and amidine groups and halogen substituents (F and Cl) on the distal phenyl group. With the exception of the 3-Cl congener (**13c**), which on the other hand did not show any activity of interest, the secondary N1-isopropyl amine derivatives **13a** (X=4'-F) and **13b** (X=4'-Cl) proved to be fXa inhibitors ( $K_i$  values equal to 139 and 165 nM, respectively) more potent than the corresponding primary N1-H amine derivatives **12a** and **12b**. The guanidine derivative **14b** had 5-fold better affinity for fXa ( $K_i$  = 31 nM) compared with the corresponding N1-isopropyl derivative **13b**.

With regard to the N1-substitution, similar trends in the fXa inhibitory potency (i.e., N-amidine > N-isopropyl > N-H) were observed with the isonipecotanilide derivatives bearing 5-arylisoxazol-3-yl (**15–17**) instead of the biphenyl moiety (Table 2). The 4-Cl-phenyl derivatives **16b** and **17b** demonstrated similar potencies to **13b** and **14b** in the biphenyl series, whereas replacing the 4-Cl-phenyl group with the slightly more polar 2-Cl-thiophen-5-yl group provided about 2-fold enhanced binding affinity to fXa either for N1-isopropyl (**16e**) and N1-amidine (**17e**) derivatives. Among the N1-H derivatives, **15e** was the only compound with a submicromolar fXa  $K_i$  value.

The most potent fXa inhibitor of the *meta*-substituted series **17e** ( $K_i$  = 15 nM), that is the derivative with the N1-amidine P1 group and the 2-chlorothiophenyl P4 group, exhibited 1000-fold selectivity over thrombin and just nearly 400-fold selectivity over chymotrypsin. However, the N1-isopropyl analog **16e**, although less selective over thrombin and  $\alpha$ -CT, showed higher anticoagulant activity (PT<sub>2</sub>) than the corresponding N1-amidine derivative **17e**, suggesting a role of lipophilicity in the anticoagulant activity. Compound **16e** showed better membrane permeability than **17e** (results not shown), as assessed with PAMPA (parallel artificial membrane permeability assay) performed in conditions which allows the potential for gastrointestinal absorption of ionizable drugs to be estimated (Wohnsland and Faller, 2001; Ottaviani et al., 2008).

We finally investigated the *ortho* isomers of the compounds in Table 2, focusing the SAR exploration on the *ortho*-substituted derivatives bearing 4-Cl-phenyl and 2-Cl-thiophen-5-yl groups (Table 3).

A substantial improvement in the fXa inhibition potency of the *ortho*-substituted isonipecotanilides over the corresponding *meta* isomers was achieved with the N1-isopropyl derivatives. Notably, compound **21e** showed excellent inhibition potency in the subnanomolar range ( $K_i$  = 0.3 nM), anticoagulant activity in the low micromolar range (PT<sub>2</sub> = 3.3  $\mu$ M), and noteworthy selec-

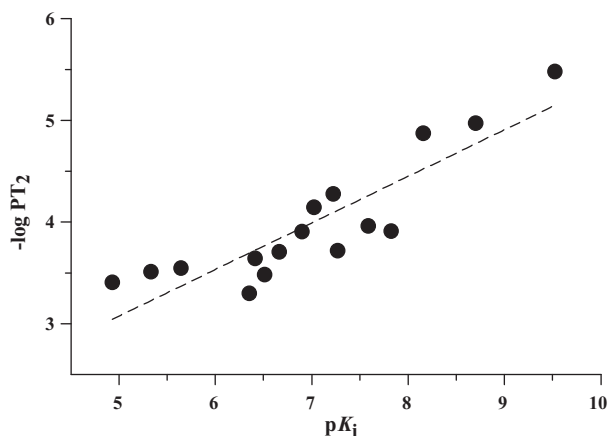


Fig. 3. Linear relationship between in vitro anticoagulant activity ( $-\log PT_2$ ) and fXa inhibitory activity ( $-\log K_i$ ) of compounds **15–22**.

tivity over thrombin and  $\alpha$ -CT (selectivity ratios of 36700 and 200000, respectively), as well as over other assayed serine proteases, namely the blood coagulation factor VIIa, trypsin and human leucocyte elastase (no significant inhibition at 250  $\mu$ M concentration). The binding affinity for fXa of the *ortho* isomer **21e** strongly enhanced compared with the *meta* isomer **16e**, being the estimated change in free energy of binding ( $\Delta\Delta G$ ) approximately equal to  $-3.4 \text{ kcal mol}^{-1}$  and the related increase in  $PT_2$  higher than 20-fold. In the *ortho*-substituted series, both the guanidine derivatives **22b** and **22e** showed lower affinity (and selectivity) for fXa than that of the corresponding N1-*i*Pr derivatives **21b** and **21e**, and thus a 3–4-fold drop in the  $PT_2$  parameter. Taking into account all the available data, the  $PT_2$  parameter and fXa inhibition constant, both in log units, resulted in a pretty correlation (Fig. 3) with a determination coefficient ( $r^2$ ) equal to 0.780:

$$-\log PT_2 = 0.46(\pm 0.06) pK_i + 0.78(\pm 0.46)$$

$$n = 16; r^2 = 0.780; s = 0.304; F = 49.6 \quad (2)$$

The lipophilicity of the investigated compounds was assessed by hydrophilic interaction liquid chromatography (HILIC), which had proved to be suitable for accurate measures of 1-octanol/water partition coefficients ( $\log P^N$ ) of the neutral form of basic compounds (Bard et al., 2009), such as those of this study. Indeed, it had been demonstrated that on Zic-pHILIC stationary phase, the difference between two isocratic  $\log k$  values (i.e.,  $\Delta\log k_{0-95}$ , where  $k_0$  is the capacity factor measured with 100% pH 2 aqueous mobile phase and  $k_{95}$  is the capacity factor measured using a 95% (v/v) ACN-pH 2 aqueous buffer mobile phase) is well correlated with  $\log P^N$ . The  $\log P$  values calculated from HILIC data of our compounds (Tables 2 and 3) suggest lipophilicity to play a minor role in improving the anticoagulant activity. In fact, although a pairwise comparison of biological (fXa affinity and  $PT_2$ ) and  $\log P$  data between the 4-Cl-phenyl-containing compounds (**b**) and their less lipophilic 2-Cl-thiophen-5-yl analogs (**e**) would suggest a trend (i.e., the activity improves due to the increased polarity), no general relation was found between lipophilicity and anticoagulant activity. Most likely, the activity increases because of the change in the position of the chlorine atom with regard to Tyr228 in the S1 subsite (and not because of the increased polarity), as a consequence of the replacement of the 4-Cl-phenyl with the 2-Cl-thiophen-5-yl.

### 3.3. Molecular modeling

Molecular modeling studies with the GOLD software (Jones et al., 1997), successfully used by some of us in ligand- and structure-based design of serine proteases' inhibitors (Nicolotti et al., 2008, 2009, 2010), were performed by docking the inhibitor molecules into the active site of factor Xa. The X-ray crystal structure of human fXa in complex with a highly potent 1*H*-indole-2-carboxamide-based inhibitor (PDB code: 2BOH) (Nazaré et al., 2004, 2005) was retrieved and used as target structure after removing the ligand.

Docking calculations were performed with eight highly potent inhibitors ( $K_i < 100 \text{ nM}$ ), namely **14b** (Table 1), **16e**, **17b**, **17e** (Table 2), **21b**, **21e**, **22b** and **22e** (Table 3), modeled in their protonated form. It is worth saying that preliminary GOLD docking calculations carried out on our previous reference compound **5** matched the posing obtained by using QXP elsewhere (de Candia et al., 2009b) as schematically shown in Fig. 2. In Fig. 4 the GOLD top scored docking poses of **21e** (A and B), **16e** (C) and **22e** (D) are shown as representative binding models. The docking simulation of the N1-isopropyl derivative **21b** gave highly scored docking poses almost similar to that of **21e** and **16e**, whereas the guanidine-containing inhibitors **14b**, **17b**, **17e** and **22b** resulted in binding modes similar to that of **22e**.

As can be seen in Fig. 4A, in which the top scored docking pose of the strongest fXa binder **21e** ( $K_i = 0.3 \text{ nM}$ ) is shown, the neutral 2-chlorothiophene group fills the S1 pocket with the chlorine atom pointing toward the center of the Tyr228 phenyl ring, whereas the basic piperidine N1-isopropyl residue, in the protonated form, is buried into the S4 aryl binding pocket, where it can be involved in efficient cation- $\pi$  interactions with the side chains of Phe174, Tyr99 and Trp215. As predicted by our modeling study and in good agreement with recent findings (Salonen et al., 2009), the tertiary ammonium head is positioned in the center of the S4 aromatic box. The *meta*-substituted isomer **16e**, albeit being a weaker binder ( $K_i = 95 \text{ nM}$ ) adopts a binding mode (Fig. 4C) similar to that of **21e**, with the chlorothiophene in S1 and the protonated N1-*i*Pr group in S4 pocket. The loss of the free energy of binding of the *meta* compared to the *ortho* isomer ( $\Delta\Delta G = 3.4 \text{ kcal mol}^{-1}$ ) could most likely result from the repositioning of the anilide scaffold which, as a consequence, does not allow the tertiary ammonium head to achieve efficient cation- $\pi$  interactions, which need the cationic  $N^+$  center to be positioned on the normal crossing the centroids of the aromatic rings (Salonen et al., 2009). As our computational data proved, the free energy costs for achieving such a binding configuration are lower for the *ortho*-substituted derivative **21e** compared to the *meta* isomer **16e**.

In contrast, compound **22e** ( $K_i = 2 \text{ nM}$ ), as well as all the other guanidine derivatives **14b**, **17b**, **17e** and **22b**, in the high-scored docking solutions binds in the opposite way, with guanidine group interacting with the Asp189 side chain at the bottom of S1 pocket and the biaryl moiety embedded into the S4 aromatic box.

In summary, suitable modifications introduced into the structure of previously reported lipophilic biphenyl-containing isonipicotanylides (de Candia et al., 2009b) enhanced their fXa affinity, while lowering their lipophilicity by about 2  $\log P$  units. In particular, some N1-isopropyl *ortho*-substituted isonipicotanylides, bearing privileged oral bioavailability-mediating 5-(chloroaryl)isoxazol-3-yl groups (Pinto et al., 2010), have been identified as highly potent and selective fXa inhibitors. Among them, the chlorothiophene-bearing compound **21e** ( $K_i = 0.3 \text{ nM}$ ) is the most potent and selective fXa inhibitor, endowed with good anticoagulant activity as assessed by the PT clotting assay ( $PT_2 = 3.3 \mu\text{M}$ ).

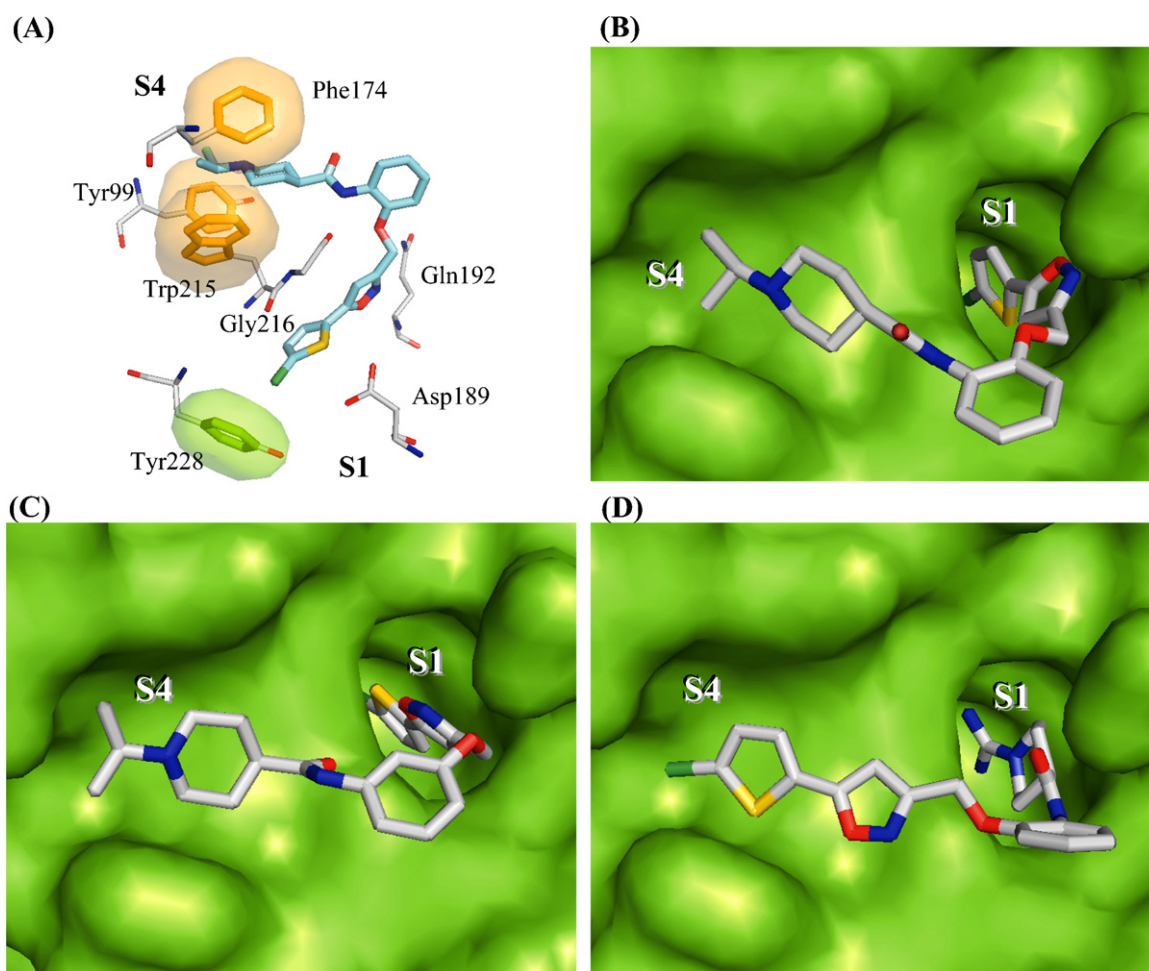


**Fig. 4.** GOLD highest scored docking poses of 5-(5-chlorothien-2-yl)isoxazole-containing isonipecotanilide inhibitors **21e** (A and B,  $K_i = 0.3$  nM), **16e** (C,  $K_i = 95$  nM) and **22e** (D,  $K_i = 2$  nM) into the binding pocket of human fXa (PDB code: 2BOH). (A) Stick representation of **21e** (carbon atoms in cyan) bound to fXa, with key amino acids in the S1 and S4 binding sites; hydrogen atoms are omitted for clarity and Van der Waals surfaces of the aromatic residues are shown. Representation of the docking modes of **21e** (B), **16e** (C) and **22e** (D) wherein the protein is rendered with the green-colored surface. The figure was drawn by PyMOL. (For interpretation of the references to color in this figure legend, the reader is referred to the web version of the article.)

Some of the observed changes in fXa affinity and in vitro anti-coagulant activity could also result from changes in lipophilicity, which in this study has been measured by hydrophilic interaction liquid chromatography (HILIC), but the log *P*-related parameters show that lipophilicity plays a minor role. Molecular modeling studies were instead helpful in understanding the SARs obtained.

As predicted by docking calculations, and in good agreement with the available X-ray crystallographic structures of fXa/inhibitor complexes (Nazaré et al., 2005), depending upon the substituent appended at the piperidine nitrogen (N1), the isonipecotamide-based fXa inhibitors examined herein can achieve two different binding modes. The N1-isopropyl derivatives (e.g., **21e**) preferably direct the neutral 2-chlorothiophene group into the S1 pocket, wherein the chlorine atom points toward the center of the Tyr228 phenyl ring, and the tertiary ammonium head (i.e., the protonated N1-*i*Pr residue) into the S4 box, where it undergoes efficient cation- $\pi$  interactions, and additional favorable C-H... $\pi$  interactions by the isopropyl group as well, with the side chains of Phe174, Tyr99 and Trp215. Despite a similar binding mode, the *meta*-substituted derivative **16e** is a fXa inhibitor weaker than the *ortho* isomer **21e** ( $\Delta\Delta G = 3.4$  kcal mol<sup>-1</sup>) due to a less efficient cation- $\pi$  interactions. In contrast, the guanidine derivatives (e.g., **22e**) adopt an opposite binding mode, with the guanidinium group interacting with the Asp189 carboxylate at the bottom of S1 pocket and the

biaryl moiety most likely engaged in hydrophobic interactions with the aromatic residues of the S4 cavity. The same opposite binding mode was predicted for the N1-H derivative **20e**, which however is a fXa binder weaker than **22e** ( $\Delta\Delta G = 1.9$  kcal mol<sup>-1</sup>).

Compound **21e** has been chosen as the lead from this class of biarylmethoxy isonipecotanilide fXa inhibitors for further modifications, which will be designed exploiting the SARs and the molecular modeling results obtained in this study.

#### Acknowledgment

C.A. acknowledges the financial support by the Italian Ministry for Education Universities and Research (MIUR, Rome, Italy); PRIN 2007, grant no. 2007T9HTFB.003.

#### Appendix A. Supplementary data

Supplementary data associated with this article can be found, in the online version, at doi:10.1016/j.ejps.2010.11.010.

#### References

- Al-Obeidi, F., Ostrem, J.A., 1999. Factor Xa inhibitors. *Expert Opin. Ther. Patents* 9, 931–953.

- Ansell, J., 2007. Factor Xa or thrombin: is factor Xa a better target? *J. Thromb. Haemostasis* 5 (Suppl. 1), 60–64.
- Appel, R., 1975. Tertiary phosphane/tetrachloromethane, a versatile reagent for chlorination, dehydration, and P–N linkage. *Angew. Chem., Int. Ed.* 14, 801–811.
- Areppally, G.M., Ortel, T.L., 2006. Heparin-induced thrombocytopenia. *N. Engl. J. Med.* 355, 809–817.
- Bard, B., Carrupt, P.-A., Martel, S., 2009. Lipophilicity of basic drugs measured by hydrophilic interaction chromatography. *J. Med. Chem.* 52, 3416–3419.
- Böhm, M., Stürzebecher, J., Klebe, G., 1999. Three-dimensional quantitative structure–activity relationship analyses using comparative molecular field analysis and comparative molecular similarity indices analysis to elucidate selectivity differences of inhibitors binding to trypsin, thrombin, and factor Xa. *J. Med. Chem.* 42, 458–477.
- Cheng, Y., Prusoff, W.H., 1973. Relationship between the inhibition constant ( $K_i$ ) and the concentration of inhibitor which causes 50% inhibition ( $IC_{50}$ ) of an enzymatic reaction. *Biochem. Pharmacol.* 22, 3099–3108.
- de Candia, M., Lopopolo, G., Altomare, C., 2009a. Novel factor Xa inhibitors: a patent review. *Expert Opin. Ther. Patents* 19, 1535–1580.
- de Candia, M., Liantonio, F., Carotti, A., De Cristofaro, R., Altomare, C., 2009b. Fluorinated benzyloxyphenyl piperidine-4-carboxamides with dual function against thrombosis: inhibitors of factor Xa and platelet aggregation. *J. Med. Chem.* 52, 1018–1028.
- Guillot, A., 2010. Development of experimental methods to determine high lipophilicity of new chemical compounds. Ph.D. Thesis, Applications to Cyclosporin A and Bioconcentration. School of pharmaceutical sciences, University of Geneva, University of Lausanne.
- Haginoya, N., Kobayashi, S., Komoriya, S., Hirokawa, Y., Furugori, T., Nagahara, T., 2004. Orally active factor Xa inhibitors: 4,5,6,7-tetrahydrothiazolo[5,4-c]pyridine derivatives. *Bioorg. Med. Chem. Lett.* 14, 2935–2939.
- Jones, G., Willett, P., Glen, R.C., Leach, A.R.L., Taylor, R., 1997. Development and validation of a genetic algorithm for flexible docking. *J. Mol. Biol.* 267, 727–748.
- Krynetskiy, E., McDonnell, P., 2007. Building individualized medicine: prevention of adverse reactions to warfarin therapy. *J. Pharmacol. Exp. Ther.* 322, 427–434.
- Lam, P.Y., Clark, C.G., Li, R., Pinto, D.J., Orwat, M.J., Galemmo, R.A., Fevig, J.M., Teleha, C.A., Alexander, R.S., Smallwood, A.M., Rossi, K.A., Wright, M.R., Bai, S.A., He, K., Luettgen, J.M., Wong, P.C., Knabb, R.M., Wexler, R.R., 2003. Structure-based design of novel guanidine/benzamide mimics: potent and orally bioavailable Factor Xa inhibitors as novel anticoagulants. *J. Med. Chem.* 46, 4405–4418.
- Leadley, R.J., 2001. Coagulation factor Xa inhibition: biological background and rationale. *Curr. Top. Med. Chem.* 1, 151–159.
- Liu, W.J., Xie, Y.X., Liang, Y., Li, J.H., 2006. Reusable and efficient Pd(OAc)<sub>2</sub>/TBAB/PEG-400 system for Suzuki–Miyaura cross-coupling reaction under ligand-free condition. *Synthesis* 5, 860–864.
- Lumma Jr., W.C., Witherup, K.M., Tucker, T.J., Brady, S.F., Sisko, J.T., Naylor-Olsen, A.M., Lewis, S.D., Lucas, B.J., Vacca, J.P., 1998. Design of novel, potent, noncovalent inhibitors of thrombin with nonbasic P1 substructures: rapid structure–activity studies by solid-phase synthesis. *J. Med. Chem.* 1998, 1011–1013.
- Mackman, N., 2008. Triggers, targets and treatment for thrombosis. *Nature* 451, 914–918.
- Maignan, S., Mikol, V., 2001. The use of 3D structural data in the design of specific factor Xa inhibitors. *Curr. Top. Med. Chem.* 1, 161–174.
- Maignan, S., Guillotheau, J.P., Choi-Sledeski, Y.M., Becker, M.R., Ewing, W.R., Pauls, H.W., Spada, A.P., Mikol, V., 2003. Molecular structures of human factor Xa complexed with ketopiperazine inhibitors: preference for a neutral group in the S1 pocket. *J. Med. Chem.* 46, 685–690.
- McMartin, C., Bohacek, R.S., 1997. QXO: powerful, rapid computer algorithms for structure-based drug design. *J. Comput. Aided Mol. Des.* 11, 333–344.
- Miguez, J.M.A., Adrio, L.A., Sousa-Pedrares, A., Vila, J.M., Hii, K.K., 2007. A practical and general synthesis of unsymmetrical terphenyls. *J. Org. Chem.* 72, 7771–7774.
- Mitsunobu, O., 1981. The Use of Diethyl Azodicarboxylate and Triphenylphosphine in Synthesis and Transformation of Natural Products. *Synthesis*, 1–28.
- Murcia, M., Morreale, A., Ortiz, A.R., 2006. Comparative binding energy analysis considering multiple receptors: a step toward 3D-QSAR models for multiple targets. *J. Med. Chem.* 49, 6241–6253.
- Nazaré, M., Essrich, M., Will, D.W., Matter, H., Ritter, K., Urmann, M., Bauer, A., Schreuder, H., Dudda, A., Czech, J., Lorenz, M., Laux, V., Wehner, V., 2004. Factor Xa inhibitors based on a 2-carboxyindole scaffold: SAR of neutral P1 substituents. *Bioorg. Med. Chem. Lett.* 14, 4191–4195.
- Nazaré, M., Will, D.W., Matter, H., Schreuder, H., Ritter, K., Urmann, M., Essrich, M., Bauer, A., Wagner, M., Czech, J., Lorenz, M., Laux, V., Wehner, V., 2005. Probing the subpockets of factor Xa reveals two binding modes for inhibitors based on a 2-carboxyindole scaffold: a study combining structure–activity relationship and X-ray crystallography. *J. Med. Chem.* 48, 4511–4525.
- Nicolotti, O., Miscioscia, T.F., Carotti, A., Leonetti, F., Carotti, A., 2008. An integrated approach to ligand- and structure-based drug design: development and application to a series of serine protease inhibitors. *J. Chem. Inf. Model.* 48, 1211–1226.
- Nicolotti, O., Giangreco, I., Miscioscia, T.F., Carotti, A., 2009. Improving quantitative structure–activity relationships through multiobjective optimization. *J. Chem. Inf. Model.* 49, 2290–2302.
- Nicolotti, O., Giangreco, I., Miscioscia, T.F., Convertino, M., Leonetti, F., Pisani, L., Carotti, A., 2010. Screening of benzamide-based thrombin inhibitors via a linear interaction energy in continuum electrostatics models. *J. Comput. Aided Mol. Des.* 24, 117–129.
- Nissink, J.W., Murray, C., Hartshorn, M., Verdonk, M.L., Cole, J.C., Taylor, R., 2002. A new test set for validating predictions of protein–ligand interaction. *Proteins* 49, 457–471.
- Ottaviani, G., Martel, S., Escarala, C., Nicolle, E., Carrupt, P.-A., 2008. The PAMPA technique as a HTS tool for partition coefficients determination in different solvent/water systems. *Eur. J. Pharm. Sci.* 35, 68–75.
- Pinto, D.J.P., Orwat, M.J., Wang, S., Fevig, J.M., Quan, M.L., Amparo, E., Cacciola, J., Rossi, K.A., Alexander, R.S., Smallwood, A.M., Luettgen, J.M., Liang, L., Augst, B.J., Wright, M.R., Knabb, R.M., Wong, P.C., Wexler, R.R., Lam, P.Y.S., 2001. Discovery of 1-[3-(aminomethyl)phenyl]-N-[3-fluoro-20-(methylsulfonyl)-[1,10-biphenyl]-4-yl]-3-(trifluoromethyl)-1H-pyrazole-5-carboxamide (DPC423), a highly potent, selective, and orally bioavailable inhibitor of blood coagulation factor Xa. *J. Med. Chem.*, 566–578.
- Pinto, D.J., Orwat, M.J., Koch, S., Rossi, K.A., Alexander, R.S., Smallwood, A., Wong, P.C., Rendina, A.R., Luettgen, J.M., Knabb, R.M., He, K., Xin, B., Wexler, R.R., Lam, P.Y.S., 2007. Discovery of 1-(4-methoxyphenyl)-7-oxo-6-(4-(2-oxopiperidin-1-yl)phenyl)-4,5,6,7-tetrahydro-1H-pyrazolo[3,4-c]pyridine-3-carboxamide (apixaban, BMS-562247), a highly potent, selective, efficacious, and orally bioavailable inhibitor of blood coagulation factor Xa. *J. Med. Chem.* 50, 5339–5356.
- Pinto, D.J.P., Smalheer, J.M., Cheney, D.L., Knabb, R.M., Wexler, R.R., 2010. Factor Xa inhibitors: next-generation antithrombotic agents. *J. Med. Chem.* 53, 6243–6274.
- Quan, M.L., Lam, P.Y., Han, Q., Pinto, D.J., He, M.Y., Li, R., Ellis, C.D., Clark, C.G., Teleha, C.A., Sun, J.H., Alexander, R.S., Bai, S., Luettgen, J.M., Knabb, R.M., Wong, P.C., Wexler, R.R., 2005. Discovery of 1-(3'-aminobenzisoxazol-5'-yl)-3-trifluoromethyl-N-[2-fluoro-4-[(2-dimethylaminomethyl)imidazol-1-yl]phenyl]-1H-pyrazole-5-carboxamide hydrochloride (razaxaban), a highly potent, selective, and orally bioavailable factor Xa inhibitor. *J. Med. Chem.* 48, 1729–1744.
- Remko, M., 2009. Molecular structure, lipophilicity, solubility, absorption, and polar surface area of novel anticoagulant agents. *J. Mol. Struct. Theoret. Chem.* 916, 76–85.
- Roehrig, S., Straub, A., Pohlmann, J., Lampe, T., Pernerstorfer, J., Schlemmer, K.H., Reinemer, P., Perzborn, E., 2005. Discovery of the novel antithrombotic agent 5-chloro-N-((5S)-2-oxo-3-[4-(3-oxomorpholin-4-yl)phenyl]-1,3-oxazolidin-5-yl)methylthiophene-2-carboxamide (BAY59-7939): an oral, direct factor Xa inhibitor. *J. Med. Chem.* 48, 5900–5908.
- Roses, M., Bosch, E., 2002. Influence of mobile phase acid–base equilibria on the chromatographic behavior of protolytic compounds. *J. Chromatogr. A* 982, 1–30.
- Salonen, L.M., Bucher, C., Banner, D.W., Haap, W., Mary, J.-L., Benz, J., Kuster, O., Seiler, P., Schweizer, W.B., Diederich, F., 2009. Cation– $\pi$  interactions at the active site of factor Xa: dramatic enhancement upon stepwise N-alkylation of ammonium ions. *Angew. Chem., Int. Ed.* 48, 811–814.
- USEPA, 2007. Estimation Program Interfaces Suites (EPI Suite). Version 3.2. US Environmental Protection Agency, Washington, DC, <http://www.epa.gov/opptintr/exposure/docs/episuite.htm>.
- Van Duzer, J.H., Roland, D.M., 1994. Indolyl substituted hydroxylamine derivatives. U.S. Pat. No. 5,350,761.
- Verdonk, M.L., Cole, J.C., Hartshorn, M.J., Murray, C.W., Taylor, R.D., 2003. Improved protein–ligand docking using GOLD. *Proteins* 52, 609–623.
- Weitz, J.I., Linkins, L.A., 2007. Beyond heparin and warfarin: the new generation of anticoagulants. *Expert Opin. Invest. Drugs* 16, 271–282.
- Wohnsland, F., Faller, B., 2001. High-throughput permeability pH profile and high-throughput alkane/water log P with artificial membranes. *J. Med. Chem.* 44, 923–930.
- Wong, P.C., Crain, E.J., Watson, C.A., Xin, B., 2009. Favorable therapeutic index of the direct factor Xa inhibitors, apixaban and rivaroxaban, compared with the thrombin inhibitor dabigatran in rabbits. *J. Thromb. Haemostasis* 7, 1313–1320.